



Fast and real-time observation of hydrogen absorption kinetics for palladium nanoparticles

Daiju Matsumura*, Yuka Okajima, Yasuo Nishihata, Jun'ichiro Mizuki

Quantum Beam Science Directorate, Japan Atomic Energy Agency, 1-1-1 Koto, Sayo, Hyogo 679-5148, Japan

ARTICLE INFO

Article history:

Received 22 July 2010

Received in revised form 7 October 2010

Accepted 18 October 2010

Available online 3 November 2010

Keywords:

Nanostructured materials

Gas–solid reactions

Kinetics

X-ray and gamma-ray spectroscopies

ABSTRACT

Structural change of Pd nanoparticles on aluminum oxide during hydrogen absorption reaction was directly observed by X-ray absorption fine structure with dispersive optics. Hydrogen pressure dependence of the expansion of the interatomic distance for Pd–Pd bonding in Pd nanoparticles was investigated by real-time-resolved and *in situ* observation with a rate of 50 Hz at room temperature. It has been revealed that the Pd nanoparticles show strong hydrogen pressure dependence of the reaction rate and the saturated interatomic distance for the hydrogen absorption. Determined reaction order implies that the rate of the hydrogen absorption reaction is limited by the surface dissociative adsorption step.

© 2010 Elsevier B.V. All rights reserved.

1. Introduction

Palladium is the classical hydrogen storage material because of the small activation barrier for the surface adsorption and the exothermal reaction for the inner absorption. H atoms are absorbed into the octahedral interstitials of Pd fcc crystal and elongate the Pd–Pd interatomic distance. Absorption isotherms for Pd–H system indicate that the hydrogen absorption occurs in the wide ranges of pressure and temperature. However, there are still open questions about the kinetics of the absorption process, for example, determination of the limiting rate step [1–3]. Most of studies about the kinetics of the hydrogen absorption process deal with the hydrogen pressure as an observation method. It is important to study from the viewpoint of the storage material in order to understand the real interaction between the hydrogen gas and the storage material. Direct observation of the atomic and electronic structure of Pd metal during the hydrogen absorption reaction, which consists of the surface adsorption and the following inner penetration processes, can bring about the new understandings for the metal–gas interaction.

Pd nanoparticles as hydrogen storage materials have attracted much attention because hydrogen absorption properties of the nanoparticles differ from those of the bulk materials [4–8]. Metal particles with a diameter of nanometers are usually used for the catalysts with an advantage of the large surface area as a reaction

field. However, the large surface and interface areas can influence the electronic and structural properties of the materials and change the hydrogen absorption property. As for the Pd–H system, the low-concentration phase shows the solid-solution (α phase), while the high-concentration phase shows the metal hydride with largely expanded lattice (β phase). Although there is a significant phase boundary between α and β phases in the bulk Pd, the Pd metal fine particles show smooth change between the two phases. For the explanation of the characteristic property of hydrogen absorption in the Pd metal fine particles, surface effect and size effect were suggested [4,9,10]. Kinetic study for the Pd nanoparticles during the hydrogen absorption reaction helps us know the origin of the characteristic property of the nanoparticles.

In this paper, the time-resolved structural change of Pd metal nanoparticles during hydrogen absorption reaction by X-ray absorption fine structure (XAFS) spectra with dispersive mode is presented [11]. The XAFS technique has an advantage for the observation of the supported materials with a feature of the element selective and the local sensitive properties. The dispersive mode, which is constructed by the curved crystal and the space-resolved detector enables us to obtain the XAFS spectra without any motion of the optics, which results in the relatively stable and fast determination of structural parameters [12]. Pressure dependent study leads to new information about the hydrogen absorption process in Pd metal nanoparticles.

2. Experiments

All the Pd *K*-edge XAFS spectra were measured by the dispersive mode at the bending magnet beamline BL14B1 and BL28B2 of SPring-8 [11,13–15]. These two beamlines have a similar optics for the dispersive mode. Dispersed X-rays were

* Corresponding author. Tel.: +81 791 58 2637; fax: +81 791 58 0311.

E-mail address: daiju@spring8.or.jp (D. Matsumura).

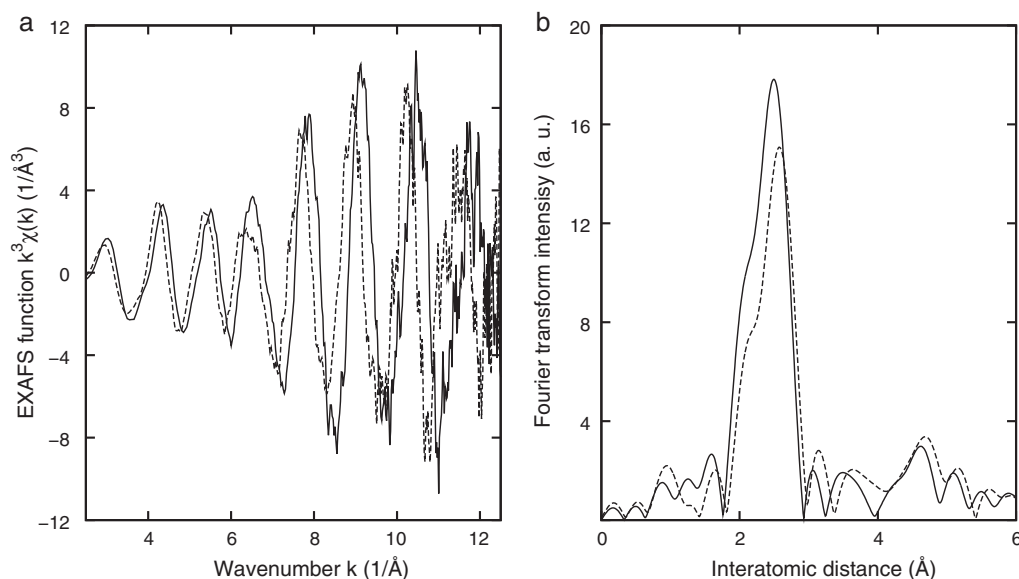


Fig. 1. (a) Pd *K*-edge EXAFS functions $k^3\chi(k)$ for Pd/Al₂O₃ before hydrogen dosing (line) and after 60 ms for hydrogen dosing at 200 kPa (dashed line). EXAFS functions were collected with dispersive mode at 50 Hz and the sampling time for each spectra is 20 ms. (b) Fourier transform intensities of EXAFS spectra in (a).

obtained from a reflection of a curved silicon crystal with a diameter of 2000 mm. The Si(422) reflection plane was used with the Laue configuration. X-rays with an energy range over 800 eV were obtained. Gd₂O₃(Tb) of 40 μ m thickness was exposed to dispersed X-rays from the sample and emitted lights were collected using a charge coupled device (CCD) camera (640 \times 480 channels, 12 bits). The intensities in the vertical direction (about 200 channels) were summed up to produce a one-dimensional spectroscopy. The horizontal focus size of the X-rays was 0.1 mm and the vertical size is equal to the sample pellet height for accumulating the intensity of transmitted X-rays. Neither the elimination of the higher harmonics nor the vertical focusing with total reflection mirrors was operated.

A powdered γ -Al₂O₃ was used in the impregnation method with dilute aqueous palladium nitric acid, Pd(NO₃)₂. Following drying and calcination at 500 °C, Pd(4 wt%)/Al₂O₃ sample was prepared. Evaluated mean diameter is 5–6 nm. The samples were reduced by hydrogen in the sample cell at 400 °C. Before the XAFS observation, the sample cell was evacuated over 30 min at room temperature in order to ensure the complete pure metal phase. After closing the valve connected to the vacuum line, hydrogen gas was stored in another inlet line. An opening signal from the valve connected to the inlet line was used to start the XAFS measurement.

The XAFS measurement of Pd nanoparticles on Al₂O₃ during H₂ dosing was operated at room temperature by 50 Hz rate (sampling time for one spectrum is 20 ms) with the real-time-resolved mode. No data accumulation by the repetition of the reaction was adopted. Because the absorbed H atoms in the Pd lattice largely elongate the interatomic distance of Pd–Pd bonding, we can observe the atomic structural change of Pd nanoparticles even at the high frame rate. All experiments were operated *in situ*.

3. Results and discussion

Fig. 1(a) demonstrates extended X-ray absorption fine structure (EXAFS) spectra for Pd/Al₂O₃ taken with dispersive mode before and after the hydrogen dosing at room temperature [11]. It is recognized that, even in the case of 50 Hz rate, the oscillation in the extended region is distinctly observed. The oscillation wavelength contracts after the hydrogen dosing, indicating the Pd–Pd interatomic distance is expanded by the hydrogen absorption. Expansion of the interatomic distance of the Pd–Pd nearest neighboring configuration is clearly shown in the Fourier transform intensities in Fig. 1(b). We cannot clearly detect higher configurations beyond the nearest neighboring shell in the Fourier transform intensities because the Pd atoms form metal nanoparticles. In order to analyze structural parameters, EXAFS curves were fitted in back-Fourier transform space [11,16]. Fourier and back-Fourier transforms were operated with the ranges of 3.0–12.0 \AA^{-1} and 1.8–2.9 \AA , respectively. Pd metal foil was employed as the reference sample. Free parameters were coordination number, interatomic

distance, and Debye–Waller factor. Those values of parameters for the reference sample at room temperature are estimated to 12, 2.75 \AA , and 0.006 \AA^2 , respectively.

Fig. 2 shows the time-resolved observation of the expansion of the Pd–Pd interatomic distance for the Pd nanoparticles with the hydrogen pressure dependence at room temperature. This figure clearly demonstrates that the hydrogen absorption rate strongly depends on the surrounding hydrogen pressure. As the hydrogen pressure increases, the reaction rate also increases, indicating the non-zero order of the chemical reaction rate. At the highest hydrogen pressure of 200 kPa in the figure, it takes only 50 ms for the complete expansion of the Pd–Pd interatomic distance. The monotonic slope of the value of the interatomic distance may be related with the result that Pd undergoes smooth change from α to β phase in nanoparticles. The Pd nanoparticles directly change to β phase without duration time of coexistence of α and β phases. The figure also indicates that the saturated value of the interatomic

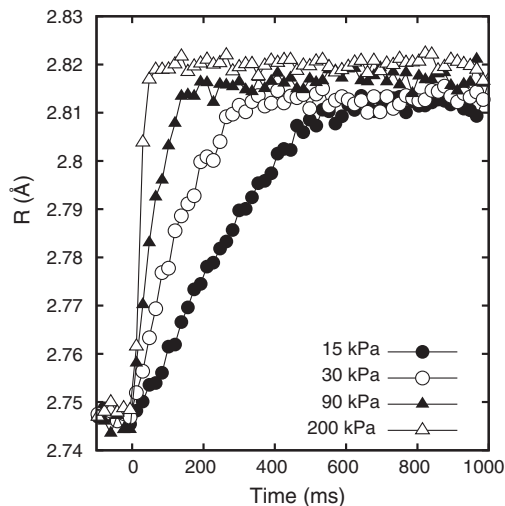


Fig. 2. Hydrogen pressure dependence of the change of the Pd–Pd interatomic distance for Pd/Al₂O₃ at room temperature. The interatomic distances were determined from the EXAFS spectra measured by the dispersive mode at 50 Hz. Operated hydrogen pressure is 15 kPa (solid circle), 30 kPa (open circle), 90 kPa (solid triangle), and 200 kPa (open triangle).

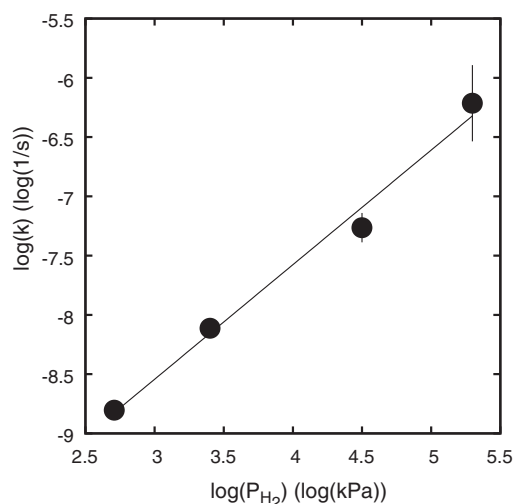


Fig. 3. Hydrogen pressure dependence of the chemical initial reaction rate k . The data are fitted to determine the reaction order. The reaction order is estimated to 0.97 ± 0.07 .

distance also depends on the surrounding hydrogen pressure. As the hydrogen pressure increases, the saturated value of the interatomic distance increases. Although a sudden change to β phase occurs in the bulk Pd, nanoparticle Pd shows a smooth change to β phase with a change of hydrogen pressure. The observed two hydrogen pressure dependences which are the reaction rate and the saturated interatomic distance clearly suggest that the interatomic distance directly reflects the hydrogen absorption property of the Pd nanoparticle.

The hydrogen pressure dependences of the reaction rate and the saturated interatomic distance were plotted in Figs. 3 and 4. Under the assumption that the absorption reaction is constructed by the one chemical reaction step, the chemical reaction order was estimated from the inverse of the half-changed time and was determined to 0.97 ± 0.07 . Normally, the hydrogen absorption process consists of the two reaction steps: the surface dissociative adsorption and the inner diffusive penetration. Because the hydrogen in the gas phase is evaluated as H_2 , if the absorption reaction rate is limited by the surface adsorption step, the chemical reaction order is evaluated to 1. On the other hand, if the hydrogen absorption reaction is limited by the inner diffusion step, because the diffusion is operated by H atom, the chemical reaction order is evaluated to 2. In this study, the determined chemical reaction order is almost

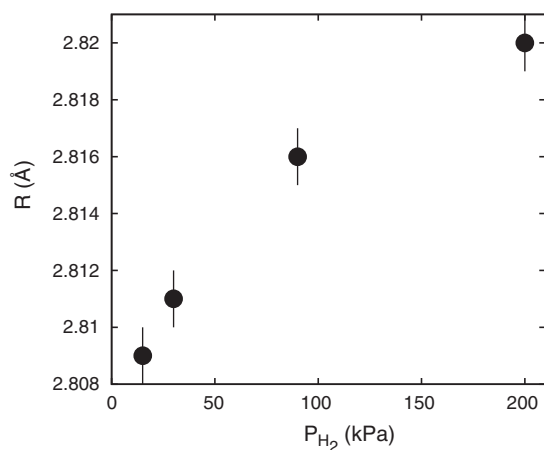


Fig. 4. Hydrogen pressure dependence of the saturation value of the Pd–Pd interatomic distance after the hydrogen dosing.

one, indicating the reaction rate of the hydrogen absorption of the Pd nanoparticle is limited by the surface dissociative adsorption step. The hydrogen pressure dependence of the saturation value of the interatomic distance shows a curve with upper convex as seen in Fig. 4. This resembles Sieverts' law showing hydrogen concentration has square-root dependence on pressure. Because this law usually holds for low-concentration metal–hydrogen systems, the Pd nanoparticles in the high-concentration hydride phase may have some properties of the low-concentration solid–solution phase.

In the case of the bulk Pd surface, although the hydrogen absorption kinetics under low pressure has been widely studied, the high-pressure experiments around the atmospheric pressure such as this study are seldom conducted [1,17]. For the clean surface of Pd, it was pointed out that the inner diffusion step limits the rate of the hydrogen absorption reaction [1]. Because the absorbed hydrogen largely elongates the interatomic distance of Pd in the hydride phase, it is deduced that the hydrogen diffusion step is more critical than the case of the low pressure study. Therefore, the hydrogen diffusion step should limit the reaction rate for the hydrogen absorption reaction in the high-pressure region. However, the surface dissociative adsorption step is the key process for the hydrogen absorption reaction in this study. Two reasons are considered for the change of the step limiting rate. One is the difference of the surface in nanoparticle and the single crystal. There are many steps and kinks in the surface of nanoparticle, which may change the surface dissociative adsorption property of Pd nanoparticles [18]. Another is the change of the diffusive penetration rate of the hydrogen in the nanoparticles. Because the size of the particles is a nanometer range, the penetration mechanism can be influenced by the size [8]. In order to examine these assumptions, we will try the size-dependent study of the hydrogen reaction kinetics of Pd nanoparticle in the future.

4. Conclusion

Local structural change of Pd nanoparticles on alumina surface during hydrogen absorption was continuously observed by X-ray absorption fine structure spectroscopy with dispersive mode. *In situ* and real-time-resolved observation enabled us to precisely determine the Pd–Pd interatomic distance even in the case of 50 Hz study. Pd nanoparticles directly change to the hydride phase in 50 ms at 200 kPa of hydrogen pressure. In the hydrogen pressure dependence study, both of the reaction rate and the saturation value of the interatomic distance depend on the surrounding hydrogen pressure. Kinetic analysis reveals that the surface dissociative adsorption process limits the rate of the hydrogen absorption reaction for the Pd nanoparticle.

Acknowledgements

We are grateful to Mr. K. Kato for constructing the dispersive XAFS system and stimulating discussion. We also thank to Mr. M. Taniguchi for the sample preparation. This work was supported by the New Energy and Industrial Technology Development Organization (NEDO) under “Advanced Fundamental Research Project on Hydrogen Storage Materials”.

References

- [1] B.D. Kay, C.H.F. Peden, D.W. Goodman, *Phys. Rev. B* 34 (1986) 817–822.
- [2] L.C. Fernández-Torres, E.C.H. Sykes, S.U. Nanayakkara, P.S. Weiss, *J. Chem. B* 110 (2006) 7380–7384.
- [3] T.L. Ward, T. Dao, *J. Membr. Sci.* 153 (1999) 211–231.
- [4] M. Yamauchi, R. Ikeda, H. Kitagawa, M. Takata, *J. Phys. Chem. C* 112 (2008) 3294–3299.
- [5] M. Wilde, K. Fukutani, *Phys. Rev. B* 78 (2008) 115411.
- [6] M. Wilde, K. Fukutani, M. Naschitzki, H.-J. Freund, *Phys. Rev. B* 77 (2008) 113412.

- [7] H. Kobayashi, M. Yamauchi, H. Kitagawa, Y. Kubota, K. Kato, M. Takata, J. Am. Chem. Soc. 130 (2008) 1818–1819.
- [8] A. Pundt, M. Suleiman, C. Bähz, M.T. Reetz, R. Kirchheim, N.M. Jisrawi, Mater. Sci. Eng. B 108 (2004) 19–23.
- [9] C. Sachs, A. Pundt, R. Kirchheim, M. Winter, M.T. Reetz, D. Fritsh, Phys. Rev. B 64 (2001) 075408.
- [10] J.A. Eastman, L.J. Thompson, B.J. Kestel, Phys. Rev. B 48 (1993) 84–92.
- [11] D. Matsumura, Y. Okajima, Y. Nishihata, J. Mizuki, Mater. Res. Soc. Symp. Proc. 1262 (2010) W06-10.
- [12] T. Matsushita, R.P. Phizackerley, Jpn. J. Appl. Phys. 20 (1981) 2223–2228.
- [13] Y. Okajima, D. Matsumura, Y. Nishihata, H. Konishi, J. Mizuki, AIP Conference Proc. 879 (2007) 1234–1237.
- [14] D. Matsumura, Y. Nishihata, J. Mizuki, M. Taniguchi, M. Uenishi, H. Tanaka, J. Appl. Phys. 107 (2010) 124319.
- [15] D. Matsumura, Y. Okajima, Y. Nishihata, J. Mizuki, M. Taniguchi, M. Uenishi, H. Tanaka, J. Phys.: Conf. Ser. 190 (2009) 012154.
- [16] T. Yokoyama, H. Hamamatsu, T. Ohta, EXAFSH, The University of Tokyo, version 2.4, 1998.
- [17] L. Piccolo, A. Piednoir, J.-C. Bertolini, Surf. Sci. 600 (2006) 4211–4215.
- [18] A.M. Doyle, S.K. Shaikhutdinov, S.D. Jackson, H.-J. Freund, Angew. Chem. Int. Ed. 42 (2003) 5240–5243.